ELSEVIER

Journal of Alloys and Compounds 320 (2001) 267–275

Journal of ALLOYS AND COMPOUNDS

www.elsevier.com/locate/jallcom

Thermodynamic properties and phase diagrams of the binary systems B_2O_3–Ga_2O_3, B_2O_3–Al_2O_3 and B_2O_3–In_2O_3

Michael Hoch*

Department of Materials Science and Engineering, University of Cincinnati, Cincinnati, OH 45221-0012, USA

Abstract

We calculated the binary phase diagrams B_2O_3–Ga_2O_3, B_2O_3–In_2O_3 and B_2O_3–Al_2O_3, and the Gibbs energy of formation of the binary compounds, using experimental liquidus data. The B_2O_3–Ga_2O_3 system is of industrial importance, because liquid B_2O_3, in which Ga_2O_3 is not very soluble, is used to protect GaAs during growth of single crystals of GaAs. During recovery of noble metals B_2O_3 is added to slags containing Al_2O_3 to lower the melting point and the viscosity. The B_2O_3–In_2O_3 system is of much less importance to industry. In all three systems we have a liquid miscibility gap, and also solid binary compounds, none of which melt congruently. The miscibility gaps are not surprising, because even in the B_2O_3–Bi_2O_3 system where four congruently melting compounds are present, a liquid miscibility gap exists close to B_2O_3. © 2001 Published by Elsevier Science B.V.

Keywords: Thermodynamics; Binary phase diagram; Solution model

1. Introduction

In an earlier paper we evaluated the B_2O_3–Bi_2O_3 system [1] where four congruently melting compounds are present, one still has a miscibility gap close to pure B_2O_3. Similarly, the enthalpy and Gibbs energy of mixing data in the binary B_2O_3–alkali and earth alkali metal oxides [2] show a tendency for phase separation close to pure liquid B_2O_3. We first give a short description of the Hoch–Arpshofen [3,4] solution model and of the model to calculate C_p(L−s), the difference in heat capacity between liquid and solid [5–7].

1.1. The Hoch–Arpshofen model

In an earlier paper Hoch and Arpshofen [3] derived a model for binary solutions. In a subsequent paper Hoch [4] derived the model for ternary, quaternary, and larger systems. The binary model is merely a special case of the ternary model. The model is an extension of Guggenheim's [8] treatment of solutions, combined with an adaptation of Pauling's [9] ideas of the metallic bond.

Guggenheim [8], when treating regular solutions and superlattices, speaks of 'treatment of quadruplets of sites, forming regular tetrahedra' and 'triplets of sites, forming equilateral triangles'. Guggenheim [8], however, always treats the strength of the A–B bond in the same way, regardless of what atoms are present in the complex. In our model the strength of the A–B bond depends on the number of B atoms to which the A atom bonds, or vice versa. In Pauling's [9] description of a metallic bond, the bond number is defined as the number of bonding electrons divided by the number of neighbors to which the specific atom bonds. In metallic copper, which consists of one bonding electron and 12 neighbors, the bond number is 1/12. This is a one-electron bond, which moves from one neighbor to another. In our model this idea is applied to ionic materials (ceramic) and van der Waals-type forces, in both an attractive and a repulsive mode. This idea is not extravagant because all bonds are caused by the behavior of electrons.

In a multicomponent system with the components A, B, C, D, etc. and their mole-fractions x, y, z, u, etc. the effect of the mixing function F_m (H_m, enthalpy of mixing, S_m^{ex}, excess entropy of mixing) of the binary system A–B (mole-fraction x and y) is

$$F_m = Wnx[1-(1-y)^{\{n-1\}}] \quad (1)$$

where W is the interaction parameter and n, the size of the complex, is an integer (2, 3, 4, etc). The term x is the mole-fraction of the component so that in Eq. (1) F_m is maximum (positive or negative) at $x>0.5$.

The excess Gibbs energy of mixing, G_m^{ex}, is a combina-

E-mail address: michael.hoch@uc.edu (M. Hoch).

0925-8388/01/$ – see front matter
PII: S0925-8388(00)01476-6

tion of H_m and S_m^{ex}. Eq. (1) can be applied to G_m^{ex} only if S_m^{ex} has the same n and x as H_m, or if S_m^{ex} is zero.

Eq. (1) also applies to binary systems: in a binary system

$$x + y = 1. \tag{2}$$

In our nomenclature 3,(Al) means that n is equal to 3, and x is Al.

In the multicomponent system (A–B–C–D–etc.) the other binary systems (A–C, A–D, A–etc., B–C, B–D, B–etc., C–D, C–etc., and D–etc.) contribute similarly to the thermodynamic properties of the multicomponent system.

The partial quantities derived from Eq. (1) do not change sign in a binary system when the composition changes from $x=0$ to $x=1$ or in a large system when x changes from $x=0$ to $x=1$ and y changes from $y=0$ to $y=1$.

One major advantage of our method is that by using regression analysis, we can calculate the binary interactions from the large systems and can compare them with the values calculated from binary data.

It is possible, that in a binary system on one side attractive, on the other repulsive forces are present (as in Au–Si, CaO–SiO_2). In this case two terms of Eq. (1) are needed:

$$F_m = W_1 xn[1-(1-y)^{\{n-1\}}] + W_2 ym[1-(1-x)^{\{m-1\}}] \tag{1a}$$

and

$$W_1 > 0 \text{ and } W_2 < 0 \text{ or vice versa.} \tag{3}$$

Experience [14] has shown that

$$n = 2m \text{ or } m = 2n. \tag{4}$$

Though we talk about ‘complexes’, the ideal Gibbs energy of mixing is, as in Guggenheim [8]

$$G_m^{id} = RT(x_1 \ln x_1 + x_2 \ln x_2 + x_3 \ln x_3 + \ldots). \tag{5}$$

A great advantage of our model is that we have never needed ternary interaction parameters. More important, we can obtain the binary interaction parameters from ternary or quaternary data by regression analysis; the latter must agree with data obtained from binary data.

The interaction parameters are designated depending on what experimental data they were calculated from: W_h from H_m enthalpy of mixing, W_s from S_m^{ex}, excess entropy of mixing, and W_g from G_m^{ex}, excess Gibbs energy of mixing.

In all of our calculations the thermodynamic quantities are divided by R, the gas constant. Thus the enthalpy H and the Gibbs energy G are expressed in kK (kiloKelvin); the entropy S and the heat capacity C_p are dimensionless.

1.2. Difference in heat capacity between liquid and solid $C_p(L-s)$

The Gibbs energy of fusion $G(L-s)$ at temperatures below and above the melting point, and thus the calculated phase diagram is greatly influenced by the difference in heat capacity between liquid and solid $C_p(L-s)$.

The heat capacity data of solids $C_p(s)$ and liquids $C_p(L)$ of elements and compounds, where accurate data are available, can be represented by [5–7]

$$C_p(s)/R = 3F(\Theta_D(s)/T) + bT + dT^3 \tag{6}$$

$$C_p(L)/R = 3F(\Theta_D(L)/T) + bT + hT^{-2} \tag{7}$$

where $F(\Theta_D/T)$ is the Debye function, b is the electronic contribution, and d and h are the anharmonic contributions.

In our calculations we assume that at the elevated temperatures $3F(\Theta_D(s)/T)$ and $3F(\Theta_D(L)/T)$ are equal.

We calculated $C_p(L-s)$ [6] for various materials where heat capacity or heat content data for solid and liquid were available, using Eqs. (6) and (7). We investigated 25 elements and compounds, from low melting Pb to high melting UO_2. For each material we calculated T_{glass}, the theoretical glass transition temperature, where $S(L-s)$ becomes zero, below the melting point. Below this point, the glass has a somewhat higher heat capacity than the solid. We derived an equation for T_{glass} and compared the calculated theoretical glass transition temperatures with the experimental ones, for materials where they were measured. The agreement was very good. We also found [7], that $C_p(L-s)$ in all these cases can be represented by a linear equation over a large temperature range, and we derived equations for $G(L-s)$, the difference in Gibbs energy between liquid and solid. The equation for $G(L-s)$ depends only on the enthalpy and temperature of fusion of the material. $G(L-s)$ also passes zero once below, and once above the melting point. If one assumes that the heat capacity of the liquid is constant, or decreases with increasing temperature, and the heat capacity of the solid increases with increasing temperature, each solid will have a glass transition and a jelly transition temperature, at which the entropy of the liquid becomes less than that of the solid.

The equation for $C_p(L-s)$ was found to be [8]:

$$C_p(L-s)/R = e + fT \text{ per atom} \tag{8}$$

with $e/T_{mp} = (7\pm3)$ and $(e/T_{mp})/f = -(1.081\pm0.186)$, where T_{mp} is the standard melting point, in kK (kiloKelvin).

The uncertainty in the two terms is large: however we have a check because at T_{glass} the value of $G(L-s)$ is a maximum [8]. Thus we use the equations

$$e/T_{mp} = (7 \pm p \times 3) \tag{9}$$

$$(e/T_{mp})/f = -(1.081 \pm p \times 0.186) \tag{10}$$

Table 1
Thermodynamic data for the system B_2O_3–Me_2O_3 ($BO_{1.5}$–$MeO_{1.5}$)

	Al_2O_3	Ga_2O_3	In_2O_3	B_2O_3
$S_{fus}/(R\times atom)$	1.107 [10]	1.265 [11]	1.1 [11]	0.802 [10]
T_{fus}, K	2325 [10]	2073 [11]	2183 [11]	723 [10]

Solubility of Ga_2O_3, In_2O_3 and Al_2O_3 in B_2O_3; Sajuti et al. [12], Narushima et al. [17]

$\log$ (Ga_2O_3 contents/mass%) $= -4880/T + 3.95 \pm 0.05$	(973–1573 K)
$\log$ (In_2O_3 contents/mass%) $= -9208/T + 5.32 \pm 0.09$	(1273–1573 K)
$\log$ (Al_2O_3 contents/mass%) $= -6043/T + 4.30 \pm 0.03$	(1073–1573 K)

and we adjust p so that the above condition is met. T_{glass} is given by [6]

$$(T_{glass}/T_{mp}) = 0.4018 + 0.0853 \times T_{mp}. \quad (11)$$

For application of our model we refer the reader to Refs. [1,2].

2. Results

Thermodynamic data of Ga_2O_3, In_2O_3, Al_2O_3 and B_2O_3 are given by Kubaschewski et al. [10] and Barin [11], and are reproduced in Table 1. The T_{jG} temperature, where a solid would become stable again at high temperature [6], is at 1658 K for B_2O_3. We have two partial experimental phase diagrams for the B_2O_3–Al_2O_3 binary, Fig. 308 and Fig. 2339 and a calculated one Fig. 6434 of the American Ceramic Society compilation [11]. For the B_2O_3–Ga_2O_3 and B_2O_3–In_2O_3 systems Sajuti et al. [12] give partial phase diagrams and equations for the solubility of Ga_2O_3 and In_2O_3 in liquid B_2O_3. These equations are given in Table 1. Our calculations rely very heavily on the solubility in liquid B_2O_3 of the other oxides, thus we reproduce in Fig. 1 the solubility data. The solubility data of

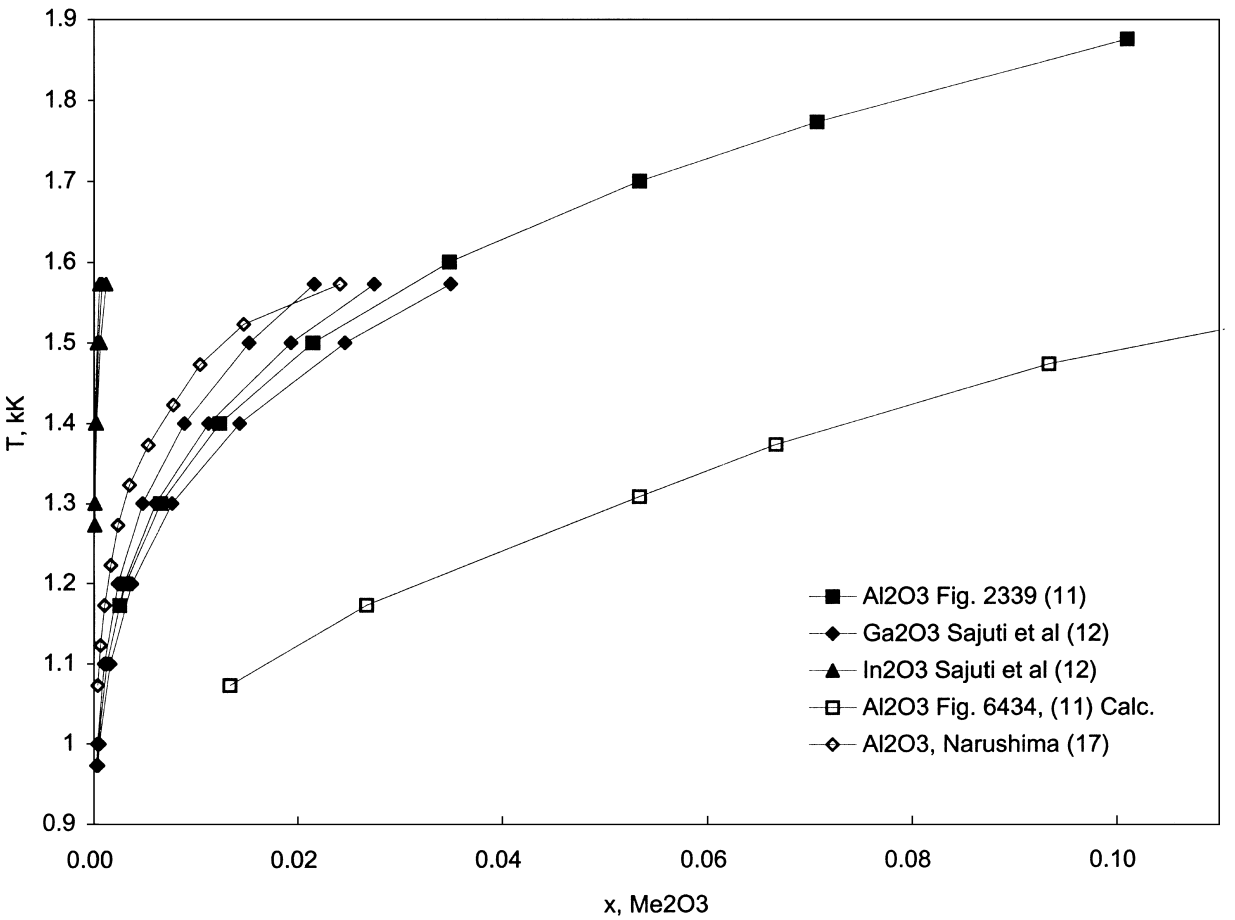

Fig. 1. Solubility of Al_2O_3, Ga_2O_3 and In_2O_3 in liquid B_2O_3. The three lines for Ga_2O_3 and In_2O_3 include plus and minus two times uncertainty of Sajuti et al. [12]. Experimental solubilities of Al_2O_3 agree. Al_2O_3 Fig. 6434 [11] does not lead to two liquid phases.

Table 2
System $BO_{1.5}$–$GaO_{1.5}$: interaction parameters, monotectic composition, enthalpy and Gibbs energy of formation of $GaBO_3$ and critical temperature and composition

Interaction parameters; all values in kK		+2×±	+2×±
W 4,($BO_{1.5}$)	0.7079±0.0624	0.7207±0.0243	0.7022±0.1076
W 2,($GaO_{1.5}$)	−1.7929±0.3621	−1.7649±0.1418	−1.8555±0.6202
R^2	0.99772	0.99969	0.99246
x_1,$GaO_{1.5}$	0.0300	0.0236	0.0382
x_2,$GaO_{1.5}$	0.51	0.517	0.506
G_{form} 0.5($BGaO_3$) at 1191 K	−0.1213±0.5167	−0.0166±0.2037	−0.2182±0.8798
x_{crit}	0.197	0.197	0.198
T_{crit} in kK	2.15	2.10	2.25

H_{form} 0.5($BGaO_3$) = −1.832±0.075 [14]
G_{form} 0.5($BGaO_3$) = −(1.832±0.075)+(1.436±0.068)×T, in kK

Al_2O_3 are given by the American Ceramic Society [13], and by Narushima et al. [17]. In the case of Ga_2O_3 and In_2O_3 we also include data with plus and minus two times the uncertainty. It is surprising that the experimental solubility of Al_2O_3 and Ga_2O_3 are almost equal, but that of In_2O_3 is much lower. We have to keep in mind, that a 1:1 compound ($GaBO_3$, $InBO_3$) is in equilibrium with liquid B_2O_3 in the case of the B_2O_3–Ga_2O_3 and B_2O_3–In_2O_3 systems, whereas a 2:1 compound, $Al_4B_2O_9$ and at high temperature a 9/11 compound, $Al_{18}B_4O_{33}$ is in equilibrium in the B_2O_3–Al_2O_3 system. The solubility in the calculated phase diagram Fig. 6434 [13,15] is much

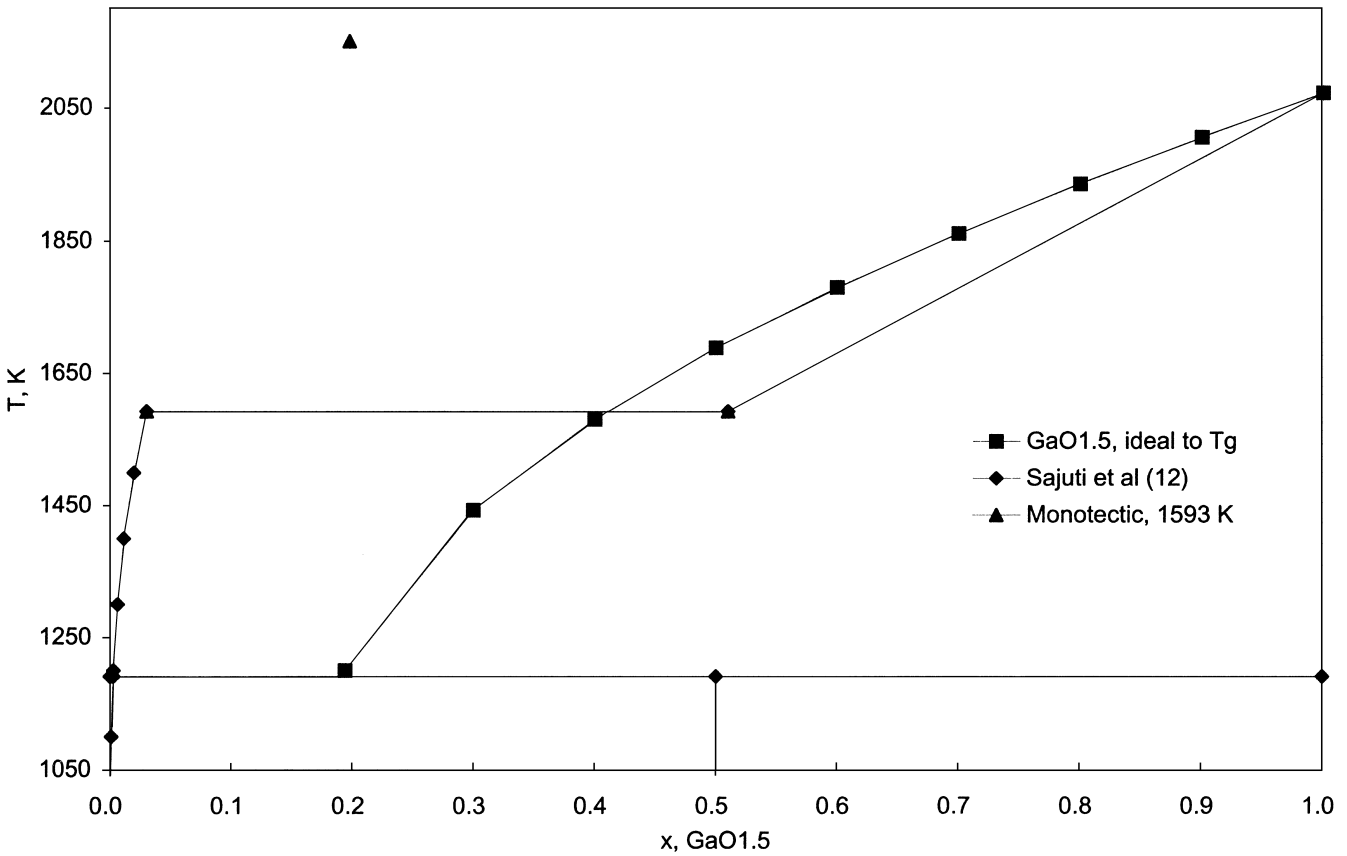

Fig. 2. Phase diagram of the binary system $BO_{1.5}$–$GaO_{1.5}$ (B_2O_3–Ga_2O_3). According to industry, GaAs solid reacts vehemently with B_2O_3 above 1560–1580. Thus two liquids. Melting point of Ga_2O_3: 2073 K, S_{fus}/(R*atom), 1.265, Barin [11]. Monotectic temperature 1.593 kK. Müller and Pelzer [14]. Critical point x, $GaO_{1.5}$ = 0.197, T_c ~ 2.150.

larger: only a large solubility permits to obtain a phase diagram with a congruently melting compound.

To calculate the phase diagrams, we need the interaction parameters. In the B_2O_3–Ga_2O_3 and B_2O_3–In_2O_3 systems [12] the stable compound is $MeO_{1.5}/BO_{1.5}=1$, thus we use an attractive parameter W_1 2,($MeO_{1.5}$) and a repulsive one W_2 4,($BO_{1.5}$). In the B_2O_3–Al_2O_3 system the stable compound is $MeO_{1.5}/BO_{1.5}=9/2$. We keep the same repulsive parameter W_2 4,($BO_{1.5}$), and, in two different calculations, use attractive parameters W_1 8,($MeO_{1.5}$) and W_1 2,($MeO_{1.5}$). As will be seen, there is no difference between the two calculations. To determine the interaction parameters and the composition of the high solubility liquid at the monotectic temperature x_2,$MeO_{1.5}$, we use four points: at the monotectic temperature the activity of $BO_{1.5}$ at the two compositions must be equal, and at each composition the activity of $MeO_{1.5}$ (referred to the solid state) must be 1. We also use the latter fact at the temperature where the compound decomposes into solid $MeO_{1.5}$ and liquid $BO_{1.5}$. We vary the composition x_2,$MeO_{1.5}$ until the regression coefficient is a maximum. The values of x_2,$MeO_{1.5}$ and that of the interaction coefficients are given in Table 2. Figs. 2–4 show the calculated phase diagrams. In all systems, the curve –■– represents the liquidus of $MeO_{1.5}$ in an ideal solution (no interaction) down to T_g, the theoretical glass transition temperature, where the entropy of the liquid becomes equal to that of the solid, and below it is less, which is impossible. In a real system, if solid compounds are present, the liquidus curve must be below the ideal one. At the temperature where the solid compound decomposes into solid $MeO_{1.5}$ and liquid $BO_{1.5}$ solution, we can calculate the Gibbs energy of formation of the compound, which should be close to zero. The uncertainty in the value is large, because in the calculation the interaction parameters have opposite signs, but in the calculation of the uncertainty they are both positive. We also calculate the critical composition and temperature; they are much less accurate than the other values.

2.1. The B_2O_3–Ga_2O_3 system

In this system, in addition to the partial phase diagram, we have from Müller and Pelzer [14] the measured monotectic temperature $T=1.593$ kK, and the enthalpy of formation of $Ga_{0.5}B_{0.5}O_{1.5}$ from solid $GaBO_{1.5}$ and liquid $BO_{1.5}$ at 0.916 kK: $\Delta H=-1.832\pm0.075$ kK. Because the monotectic temperature 1.593 kK, and the temperature

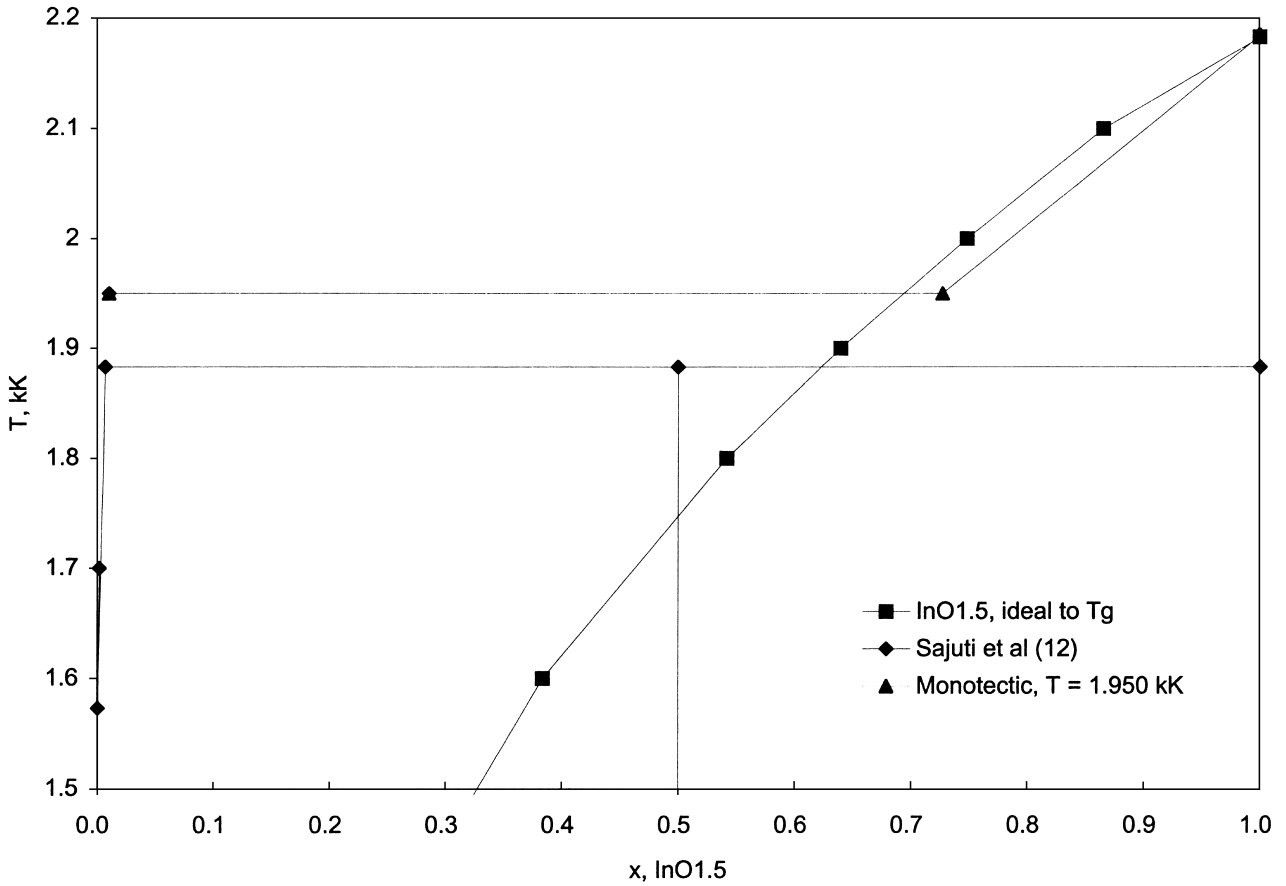

Fig. 3. Phase diagram $BO_{1.5}$–$InO_{1.5}$ (B_2O_3–In_2O_3). Miscibility gap: Monotectic temperature taken as 1950 K (between 1885 K and 2185 K). Sajuti et al. [12], solubility above 1573 K extrapolated. Critical point x, $InO_{1.5}$ 0.238, T_{cr}~3700 K.

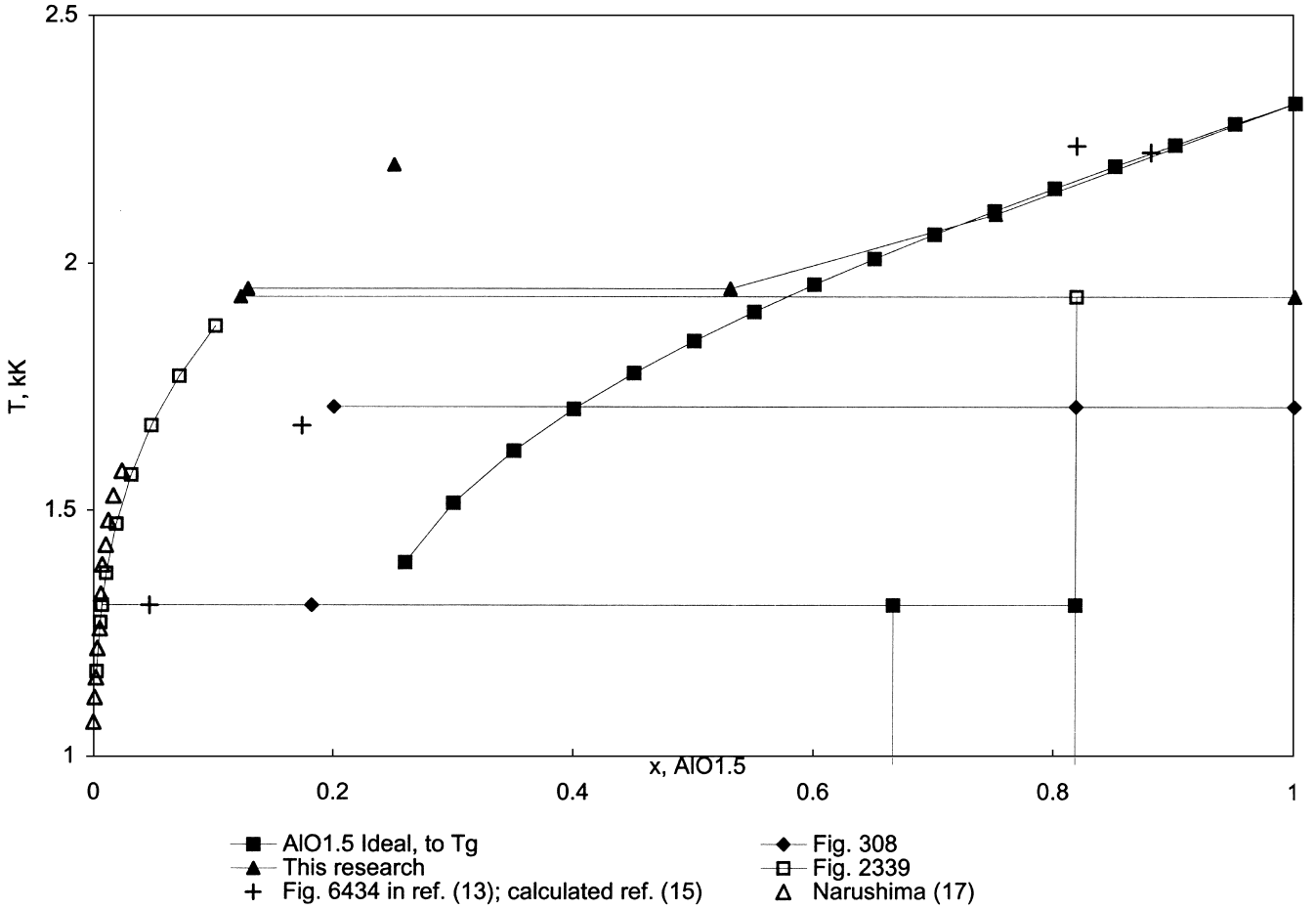

Fig. 4. Phase diagram of the binary system $BO_{1.5}$–$AlO_{1.5}$ (B_2O_3–Al_2O_3). Miscibility gap: Monotectic temperature between 1934 K and 2325 K; used 1973 K. Fig. 308 (1961); Fig. 2339 (1965) in Ref. [13]. Critical point $x_{cr}=0.2498$ $AlO_{1.5}$, $T_{cr}=2.3$ kK. This research: Decomposition temperature of $Al_{(9/11)}B_{(2/11)}O_{1.5}$.

where $Ga_{0.5}B_{0.5}O_{1.5}$ decomposes, 1.191 kK, are so far apart, we also use the solubility of $GaO_{1.5}$ in $BO_{1.5}$ at 1.5, 1.4 and 1.3 kK to determine the interaction parameters. We carried out the calculations using the thermodynamic data given in Table 1. The results are given in Table 2. We also carried out calculations using plus and minus two times the uncertainty in the solubility data. At 1.191 kK, where $GaBO_3$ decomposes into solid $GaO_{1.5}$ and a liquid solution rich in $BO_{1.5}$, we calculated the Gibbs energy of formation of $GaBO_3$. Using the interaction parameters we also calculate the critical point, also given in Table 2. Because of the ± uncertainty in the interaction parameters, the critical point data are very approximate. Otherwise there is no significant difference between the three calculations using different solubility data. Table 2 also contains the enthalpy of formation measured by Müller and Pelzer [14]. In both cases the original measurements refer to the reaction $0.5BO_{1.5}$ (L) + $0.5GaO_{1.5}$ (s) → $0.5(BGaO_3)$. From these two points we calculated the Gibbs energy change as $\Delta G=-1.832+1.436T$ in kK. Fig. 2 shows the phase diagram of the $BO_{1.5}$–$GaO_{1.5}$ binary system.

2.2. B_2O_3–In_2O_3 system

In Fig. 3 we show the results for the $BO_{1.5}$–$InO_{1.5}$ system. The calculations were similar to the B_2O_3–Ga_2O_3 system, and the data are presented in Table 3. The monotectic temperature was taken as 1.950 kK. Using the entropy change from the $BO_{1.5}$–$GaO_{1.5}$ system, we also calculated the enthalpy of formation of $0.5(BInO_3)$ from liquid $BO_{1.5}$ and solid $InO_{1.5}$: $\Delta H=-(2.741\pm0.128)$ kK. Also the Gibbs energy of formation is $\Delta G=-(2.741\pm0.128)+(1.436\pm0.068)T$ kK.

2.3. B_2O_3–Al_2O_3 system

In this system we have two partial experimental phase diagrams: Fig. 308 and 2339 [13], a calculated one, Fig. 6434 [13,15] and solubility data from Narushima et al. [17]. Fig. 4 shows the data: only the measured data of Figs. 308, 2339 and Narushima et al. [17] are drawn in solid lines. From Fig. 6434 only the eutectic point between $AlO_{1.5}$ and $Al_{0.812}B_{0.182}O_{1.5}$, the melting point of

Table 3
System $BO_{1.5}$–$InO_{1.5}$: interaction parameters, monotectic composition, Gibbs energy of formation of $InBO_3$ and critical-temperature and -composition

Interaction parameters; all values in kK		+2×±	+2×±
W 4,($BO_{1.5}$)	0.8158±0.0253	0.7155±0.0252	0.9243±0.0242
W 2,($InO_{1.5}$)	−0.5112±0.1432	−0.2542±0.1418	−0.8045±0.1371
R^2	0.99992	0.99992	0.99993
x_1,$InO_{1.5}$	0.098	0.151	0.066
x_2,$InO_{1.5}$	0.727	0.710	0.739
$T_{monotectic}$ = 1.950 kK			
G_{form} 0.5($BInO_3$) at 1883 K	−0.0367±0.2046	−0.0367±0.2009	−0.0356±0.1970
x_{crit}	0.238	0.2435	0.233
T_{crit} in kK	3.7	3.5	4.0
G_{form} 0.5($BInO_3$) = −(2.741±0.128)+(1.436±0.068)×T, in kK			

$Al_{0.812}B_{0.182}O_{1.5}$, and two points from the solubility line are shown. As already shown in Fig. 1, the calculated solubility in Fig. 6434 is much larger than the measured one in Fig. 2339 and the one from Narushima et al. [17]. Only with a high solubility, can a two-phase liquid be avoided.

Dörner et al. [15] used only the thermodynamic data of $Al_{0.667}B_{0.333}O_{1.5}$ in their calculations. We carried out the calculations as done above. We kept the repulsive interaction the same form as above W_2 4,($BO_{1.5}$). For the attractive term we used W_1 2,($BO_{1.5}$) as above, but also W_1 8,($BO_{1.5}$) because the most stable compound is $Al_{0.812}B_{0.182}O_{1.5}$. We used 1.934 kK as the temperature where $Al_{0.812}B_{0.182}O_{1.5}$ decomposes, and 1.973 kK as the monotectic temperature. At 1.308 kK $Al_{0.667}B_{0.333}O_{1.5}$ decomposes into $Al_{0.812}B_{0.182}O_{1.5}$ and $BO_{1.5}$ solution. Thus we can calculate its Gibbs energy of formation. Using the entropy term from the $B_{0.5}Ga_{0.5}O_{1.5}$, but keeping in mind that these compounds contain less $BO_{1.5}$, we use it proportionally. Table 4 contains the calculations. The numbers in the two calculations are very close, but the uncertainty ± is very different. Thus the calculation with W_1 8,($BO_{1.5}$) is the correct model. Fig. 5 shows the enthalpy of formations of $Me_{0.5}B_{0.5}O_{1.5}$ from solid $MeO_{1.5}$ and liquid $BO_{1.5}$ as a function of the ionic radius of Me^{3+}. For $AlO_{1.5}$ we use the data of $Al_{0.667}B_{0.333}O_{1.5}$. The values of $Al_{0.812}B_{0.182}O_{1.5}$ and $Al_{0.667}B_{0.333}O_{1.5}$ can be represented as a function composition with a regular solution. In Fig. 5 the value '$Al_{0.5}B_{0.5}O_{1.5}$', is calculated with the regular solution model. Finally under 'litt' we represent the average value of $Al_{0.667}B_{0.333}O_{1.5}$ from the data in Table 5. The data in Table 5 are calculated from the enthalpies of

Table 4
System $BO_{1.5}$–$AlO_{1.5}$: interaction parameters, monotectic composition, enthalpy and Gibbs energy of formation of $AlBO_3$ and critical-temperature and -composition

Interaction parameters; all values in kK	$AlO_{1.5}$	$AlO_{1.5}$
W 4,($BO_{1.5}$)	0.4460±0.0183	
W 8,($MeO_{1.5}$)	−0.0177±0.0141	
W 4,($BO_{1.5}$)		0.4403±0.0541
W 2,($MeO_{1.5}$)		−0.0714±0.2462
R^2	0.9989	0.9990
x_1,$AlO_{1.5}$	0.128	0.52
x_2,$AlO_{1.5}$	0.128	0.52
$T_{monotectic}$ = 1.973 kK		
G_{form} at 1923 K	0.0342±0.1595	−0.0392±0.6358
x_{crit}	0.2498	0.2492
T_{crit}, in kK	2.3	2.25
$H_{formation}$ from liquid $BO_{1.5}$, in kK		
$Al_{0.812}B_{0.182}O_{1.5}$	−0.9700±0.1595	−0.9709±0.6358
$Al_{0.667}B_{0.333}O_{1.5}$	−1.4859±0.1300	−1.4866±0.5181
$H_{formation}$ from solid $BO_{1.5}$, in kK		
$Al_{0.812}B_{0.182}O_{1.5}$	−0.7047±0.1595	−0.7074±0.6358
$Al_{0.667}B_{0.333}O_{1.5}$	−0.9996±0.1300	−1.0036±0.5181
$G_{formation}$ from liquid $BO_{1.5}$ and solid $AlO_{1.5}$, in kK		
$Al_{0.812}B_{0.182}O_{1.5}$	= −(0.7047±0.1595)+(0.5222±0.0247)T, in kK	
$Al_{0.667}B_{0.333}O_{1.5}$	= −(1.4859±0.1300)+(0.9572±0.0453)T, in kK	

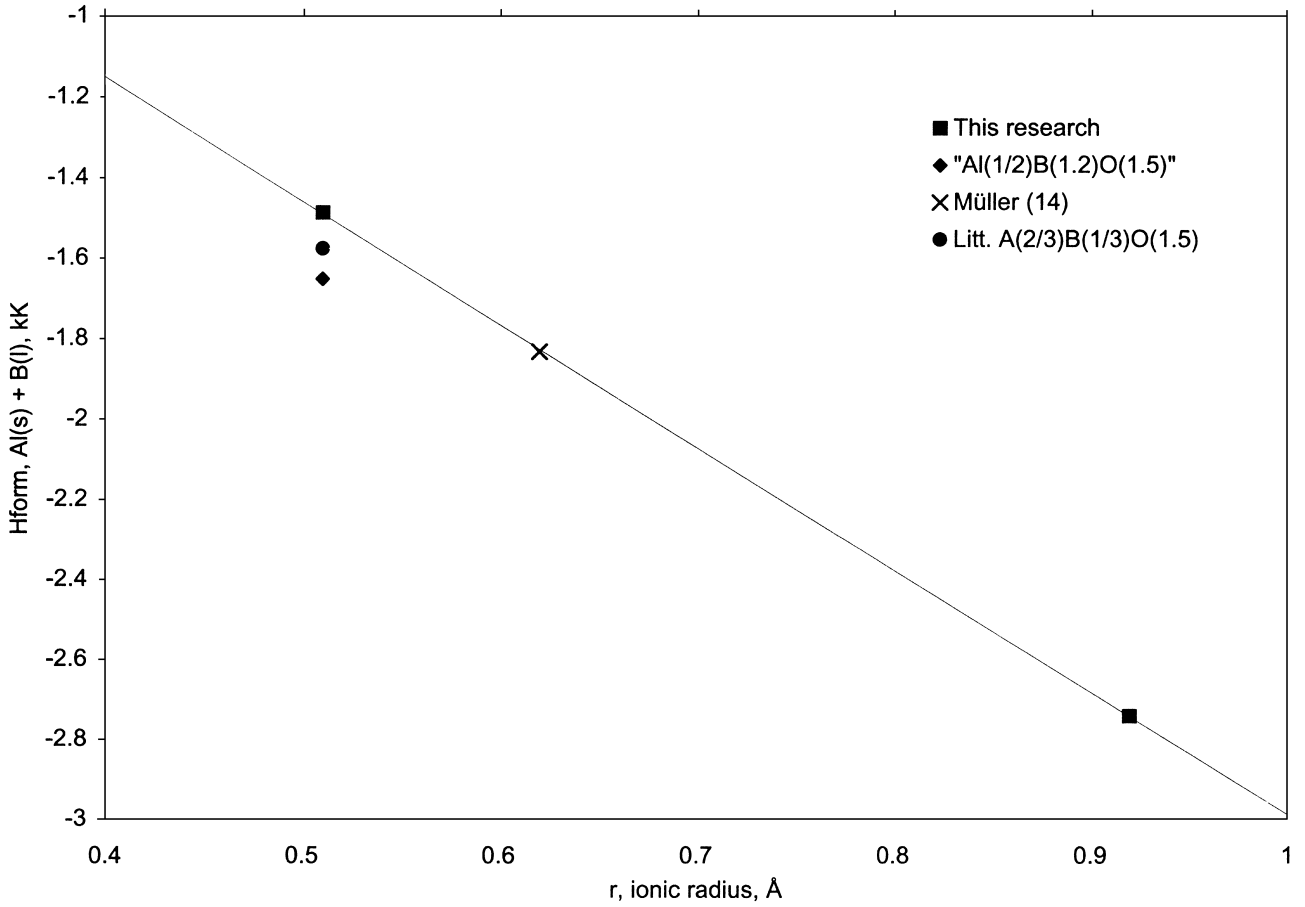

Fig. 5. Enthalpy of $BO_{1.5}$ (l). Literature: Refs. [10,11,15,16].

Table 5
Enthalpy and entropy of formation of solid $Al_xB_{(1-x)}O_{1.5}$ compounds, from solid Al_2O_3 and solid B_2O_3

Source	$Al_{0.818}B_{0.182}O_{1.5}$		$Al_{0.667}B_{0.333}O_{1.5}$	
	$\Delta H/R$, in kK	ΔS	$\Delta H/R$, in kK	ΔS
Barin et al. [16]	−0.7233	0.4803	−1.6491	0.0069
Dörner et al. [15]			−1.1262	−0.0092
Kubaschewski et al. [10]	−0.5329±0.1775	0.4806	−1.3191±0.1792	−0.0040±0.1009
Barin [11]	−0.5696	0.4949	−1.3672	−0.0113
Average	−0.6119±0.0795	−0.4786±0.0026	−1.3653±0.1870	−0.0044±0.0071
This research				
8, 4	−0.7047±0.1595		−0.9867±0.1300	
2, 4	−0.7074±0.6358		−1.0036±0.5181	

formation of the $Al_{0.5}B_{0.5}O_{1.5}$, $AlO_{1.5}$, $BO_{1.5}$ compounds from the elements. The data in Table 5 are from Barin et al. [16], Dörner et al. [15], Kubaschewski et al. [10] and Barin [11]. The agreement is good, keeping in mind that here a small difference between three large values is obtained.

3. Discussion

It may be surprising that liquid B_2O_3 and liquid Al_2O_3, Ga_2O_3 resp. In_2O_3 do not form a solution, but have a miscibility gap, though all three elements, B, Al and In are from the same group of the periodic table. The entropy of fusion of B_2O_3 is much lower than that of Al_2O_3, Ga_2O_3 and In_2O_3, and the melting point is also much lower, indicating a 'solid like structure' for liquid B_2O_3, which must be taken apart at high temperatures. The data given above in other systems [1,2] support this description.

References

[1] M. Hoch, Thermodynamics and phase diagram of the binary system Bi_2O_3–B_2O_3, Calphad 20 (4) (1996) 511–519.
[2] M. Hoch, Thermodynamics and phase diagrams in the binary

systems $Na_2O–SiO_2$, $Na_2O–GeO_2$, $Na_2O–B_2O_3$, $Li_2O–B_2O_3$, $CaO–B_2O_3$, $SrO–B_2O_3$, $BaO–B_2O_3$, J. Phase Equilibria 17 (1996) 290–301.

[3] M. Hoch, I. Arpshofen, Über ein Komplexmodell zur Berechnung der thermodynamischen Zustandsfunktionen flüssiger Legierungen, Z. Metall. 75 (1984) 23–29.

[4] M. Hoch, Application of the Hoch–Arpshofen model to ternary, quaternary and larger systems, Calphad 11 (1987) 219–224.

[5] M. Hoch, The heat capacity C_p of solids, liquids, glasses and the liquid–glass and solid–'jelly' transitions, and their influence on phase diagram calculations, High Temp.–High Press. 24 (1992) 87–96.

[6] M. Hoch, The glass–liquid and solid–jelly transition temperatures, Met. Trans. 23B (1993) 309–315.

[7] M. Hoch, The heat capacity C_p of solids and liquids, and their estimation, Z. Metall. 83 (1992) 820–823.

[8] E.A. Guggenheim, Mixtures, Clarendon Press, Oxford, 1952.

[9] L. Pauling, in: 3rd Edition, The Nature of the Chemical Bond, Cornell University Press, Ithaca, New York, 1960.

[10] O. Kubaschewski, C.B. Alcock, P.J. Spencer, in: 6th Edition, Materials Thermochemistry, Pergamon Press, New York, 1992.

[11] I. Barin, in: 3rd Edition, Thermochemical Data of Pure Substances, VCH Verlagsgesellschaft, Weinheim, Germany, 1995, Part I.

[12] D. Sajuti, M. Yano, T. Narushima, Y. Iguchi, Phase diagrams of the $Ga_2O_3–B_2O_3$ and $In_2O_3–B_2O_3$ binary systems, Mater. Trans. JIM 34 (12) (1993) 1195–1199.

[13] American Ceramic Society, Phase Diagrams for Ceramists, Vol. I–X, 1964–1996, Columbus, OH, Bi_2O_3 Fig. 323, Al_2O_3 Figs. 308, 2339, calculated Fig. 6434.

[14] H. Pelzer, F. Müller, Thermochemistry of $GaBO_3$ and phase equilibria in the $Ga_2O_3–B_2O_3$ system, J. Alloys Comp. 320 (2001) 262–266.

[15] P. Dörner, L.J. Gauckler, H. Krieg, H.L. Lukas, G. Petzow, J. Weiss, On the calculation and representation of multicomponent systems, Calphad 3 (4) (1979) 241–257.

[16] I. Barin, O. Knacke, O. Kubaschewski, Thermochemical Properties of Inorganic Substances, Supplement, Springer Verlag, Berlin, 1977.

[17] T. Narushima, D. Sajuti, K. Saeki, M. Akasaka, Y. Iguchi, private communication.